New Journal of Physics
The open–access journal for physics

Designing phoretic micro- and nano-swimmers

R Golestanian[1], T B Liverpool[2] and A Ajdari[3,4]

[1] Department of Physics and Astronomy, University of Sheffield, Sheffield S3 7RH, UK
[2] Department of Applied Mathematics, University of Leeds, Leeds LS2 9JT, UK
[3] Physico-Chimie Théorique, UMR CNRS 7083, ESPCI, 10 rue Vauquelin, 75005 Paris, France
[4] DEAS, Harvard University, 29 Oxford Street, Cambridge, MA 02138, USA
E-mail: r.golestanian@sheffield.ac.uk, t.b.liverpool@leeds.ac.uk and armand.ajdari@espci.fr

New Journal of Physics **9** (2007) 126
Received 16 January 2007
Published 15 May 2007
Online at http://www.njp.org/
doi:10.1088/1367-2630/9/5/126

Abstract. Small objects can swim by generating around them fields or gradients which in turn induce fluid motion past their surface by phoretic surface effects. We quantify for arbitrary swimmer shapes and surface patterns, how efficient swimming requires both surface 'activity' to generate the fields, and surface 'phoretic mobility.' We show in particular that (i) swimming requires symmetry breaking in either or both of the patterns of 'activity' and 'mobility,' and (ii) for a given geometrical shape and surface pattern, the swimming velocity is size-independent. In addition, for given available surface properties, our calculation framework provides a guide for optimizing the design of swimmers.

Contents

PII: S1367-2630(07)41698-6

1. Introduction

In the current miniaturization race towards small motors and engines, a rapidly expanding subdomain is the quest for autonomous swimmers, able to move in fluids which appear very viscous given the small length scales (low Reynolds number). Robotic microswimmers that generate surface distortions is an avenue (e.g. by mimicking sperms [1]), but it seems equally interesting to try to take advantage of physical phenomena that become predominant at small scales. Interfacial 'phoretic' effects (electrophoresis, thermophoresis, diffusiophoresis, [2]) by which the gradients of fields (electrostatic potential, temperature, concentration) drive the motion of colloid particles, are from this standpoint a natural avenue given the increased surface to volume ratio of smaller objects.

Very recently, in line with earlier suggestions of self-electrophoresis of objects that would be able to generate an electric field around them [2]–[4] and our recent proposal of self-diffusiophoresis [5], many experimental reports have appeared of heterogeneous objects (e.g. rods of hundreds of nanometres) swimming using different catalytic or reactive chemistry at their different ends [6]–[9]. Although many mechanisms may contribute to the observed motion [6], phoretic mechanisms have been shown to be essential for some systems [10].

In this paper we consider general self-phoretic motion, where the swimmer generates through its surface activity, gradients of (at least) a quantity (concentration of a dissolved species, electric potential, temperature), which in turn induce motion through classical interfacial phoretic processes. Because it is now possible to fabricate such objects with controlled shape and patterns of surface properties [6, 7, 11], we discuss how these design parameters affect the swimmer's velocity. A general framework is proposed to compute this velocity for arbitrary swimmer size, shape and surface pattern. We then work out explicitly a few examples for spheres and rods, geometries amenable to analytical calculations, and corresponding to existing means of fabrication [6, 7]. From these examples we extract generic rules as to the role of the pattern symmetry, of the swimmer size and shape, before concluding with a few remarks.

2. General formalism

We start with a reminder of what phoretic mechanisms are [2]. Consider e.g. a colloid in a solution where the concentration of a solute c exhibits a gradient. The colloid is then set into motion due to the induced imbalance of osmotic effects within the solid/liquid interfacial structure at the surface of the object. When the thickness of the interfacial layer is thin compared to the object, the resulting flow is most conveniently described by an effective slip velocity of the liquid past the solid at position $\mathbf{r}_s$ on the surface, proportional to the local gradient of c [2]:

$$\mathbf{v}_s(\mathbf{r}_s) = \mu(\mathbf{r}_s)(\mathbf{I} - \mathbf{nn}) \cdot \nabla c(\mathrm{r}_s) \tag{1}$$

where $\mathbf{n}$ is the local normal to the surface, $\mathbf{I}$ is the identity tensor. $\mu(\mathbf{r}_s)$ is the local 'surface phoretic mobility', positive or negative depending on specifics of the solute/surface interactions [2].

This distribution of slip on the object's surface induces a net drift velocity $\mathbf{V}$, which can be computed using the reciprocal theorem for low Reynolds-number hydrodynamics [12].[5] Its

[5] See chapter 5 of [13].

components in a basis $\{\hat{\mathbf{e}}_i\}$ are:

$$\mathbf{V}\cdot\hat{\mathbf{f}}_i = -\iint_S \mathrm{d}\mathbf{r}_s\, \mathbf{n}\cdot\boldsymbol{\sigma}_i\cdot\mathbf{v}_s, \tag{2}$$

where $\boldsymbol{\sigma}_i$ is the hydrodynamic stress tensor at the surface S of an object of the same shape dragged by an applied unit force, $\hat{\mathbf{f}}_i = \hat{\mathbf{e}}_i$ exactly equal to $\hat{\mathbf{e}}_i$, in the absence of slip.

Similar principles describe the motion of the object in a gradient of electric potential (electrophoresis), or in a temperature gradient (thermophoresis). The above formalism can be applied upon simple replacement of c by the potential ϕ_{el} or by the temperature T. For electrophoresis μ is up to a constant the so-called zeta-potential [2]. For all these situations, achieving large values of μ requires engineering of the surface in relation to the solvent (nanometre scale roughness and solvophobicity do matter! [14, 15]).

We now focus on objects that generate the gradients *themselves*, e.g. using the chemical free-energy available in the solvent [6, 7]. Returning to self-diffusiophoresis, the simplest situation corresponds to a solute generated by active sources and sinks on the surface of the object, and diffusing in the bulk. At steady-state, in the reference frame of the object, and neglecting distortions induced by the flow (small Peclet number), the solute concentration in the liquid is given by:

$$D\nabla^2 c = 0, \tag{3}$$

$$-D\mathbf{n}\cdot\nabla c(\mathbf{r}_s) = \alpha(\mathbf{r}_s), \tag{4}$$

where D is the diffusion coefficient, and $\alpha(\mathbf{r}_s)$ measures the 'surface activity' at position $\mathbf{r}_s$ on the surface, i.e. the generation or consumption of solute by a chemical reaction. In general, describing this process involves additional coupled transport problems for other species involved in the surface reactions. For simplicity, we nevertheless proceed with a fixed local value of α. This should well describe situations where the solvent contains an excess of the reactants necessary to produce and destroy the solute of interest, so that the density of active sites on the surface is what limits the fluxes. α is then this density times the rate of the chemical reaction per site [5].

For self-electrophoresis, similar formulae hold upon replacing c by ϕ_{el} and D by the solution electrical conductivity. α is then the electrical current injected by the surface. Existing realizations [9, 10] correspond to no net current generation $\iint_S \mathrm{d}\mathbf{r}_s\, \alpha(\mathbf{r}_s) = 0$, with the ions produced on one side of the swimmer and consumed on the other side, while electrons are transported through the body of the swimmer. Similarly, for thermophoresis, beyond replacing c by T and D by the thermal conductivity, the boundary condition (4) must be adjusted to account for heat transport through the object.

The general formal description (1)–(4) predicts a swimming velocity $V \sim \alpha\mu/D$, linear in the surface properties α and μ, and inversely proportional to the medium conductivity D. More interestingly, once the pattern of surface properties and the object shape are given, V is independent of the size R of the swimmer. This central point emphasizes the robustness of this swimming strategy against downsizing. In contrast, an external body force on the object scaling as $F \sim R^3$ (dielectrophoresis, magnetophoresis) leads in this viscous realm to velocities $\sim R^2$, which decrease rapidly with length scale. Further, our approach (1)–(4) allows us to relate quantitatively the velocity V to the design of the swimmer (shape, surface patterns of α and μ), as we show analytically for spheres and rods.

3. Spheres

For a sphere of radius R with a varying surface mobility, as $\mathbf{n}\cdot\sigma_i = (1/4\pi R^2)\hat{\mathbf{e}}_i$, equation (2) becomes [16]

$$\mathbf{V} = -\frac{1}{4\pi R^2}\iint_{\mathrm{S}} \mathrm{d}\mathbf{r}_{\mathrm{s}}\,\mu(\mathbf{r}_{\mathrm{s}})(\mathbf{I}-\mathbf{nn})\cdot\nabla c(\mathbf{r}_{\mathrm{s}}). \tag{5}$$

We focus further on azimuthally symmetric patterns, with surface quantities depending only on the 'latitude' angle θ with the polar axis $\hat{\mathbf{e}}_z$. We expand in Legendre polynomials. The surface activity $\alpha(\theta) = \sum_{\ell=0}^{\infty}\alpha_\ell P_\ell(\cos\theta)$, generates a concentration variation given by equations (3) and (4):

$$c(r,\theta) = c_\infty + \frac{R}{D}\sum_{\ell=0}^{\infty}\frac{\alpha_\ell}{\ell+1}\left(\frac{R}{r}\right)^{\ell+1}P_\ell(\cos\theta), \tag{6}$$

where c_∞ is the concentration at infinity. For a surface mobility $\mu(\theta) = \mu_\ell P_\ell(\cos\theta)$, the corresponding gradient yields a swimming velocity (5):

$$\mathbf{V} = -\frac{\hat{\mathbf{e}}_z}{D}\sum_{\ell=0}^{\infty}\left(\frac{\ell+1}{2\ell+3}\right)\alpha_{\ell+1}\left[\frac{\mu_\ell}{2\ell+1} - \frac{\mu_{\ell+2}}{2\ell+5}\right]. \tag{7}$$

As a first check, we recover [5] that a single active site at the pole $\alpha = \tau^{-1}\delta_{2D}(\mathbf{r}_{\mathrm{s}})$ of a sphere of uniform mobility μ yields $V = \frac{\mu}{4\pi R^2 D\tau}$. By linearity, an emitter at the back pole with rate $1/\tau_{\mathrm{e}}$ and a consumer at the front pole with rate $1/\tau_{\mathrm{c}}$, results in $V = \frac{\mu}{4\pi R^2 D}(\frac{1}{\tau_{\mathrm{e}}} + \frac{1}{\tau_{\mathrm{c}}})$.

To access useful general principles we now focus on three simple designs (figure 1), within reach of current fabrication techniques [11]. The first is the Janus sphere, with two hemispheres covered with a different enzymatic or catalytic material. Generically, their mobilities μ also differ, so we take:

$$(\alpha(\theta),\mu(\theta)) = \begin{cases}(\alpha_+,\mu_+), & 0<\theta<\frac{\pi}{2},\\ (\alpha_-,\mu_-), & \frac{\pi}{2}<\theta<\pi,\end{cases} \tag{8}$$

and find analytically

$$\mathbf{V} = \frac{1}{8}\frac{1}{D}(\alpha_- - \alpha_+)(\mu_+ + \mu_-)\hat{\mathbf{e}}_z. \tag{9}$$

This shows that symmetry breaking in the chemical activity ($\alpha_- \neq \alpha_+$) is essential to propulsion, and that the swimming velocity is larger if the two mobilities are of the same sign (which dictates the swimming direction).

The second design is a 'Saturn' particle, where the surface activity is concentrated around the equator, and where symmetry is now broken by choosing hemispheres of different mobilities. For computational convenience we solve the very similar problem defined by:

$$\alpha(\theta) = \alpha_0(1-\cos^2\theta), \quad \mu(\theta) = \mu_0\cos\theta, \tag{10}$$

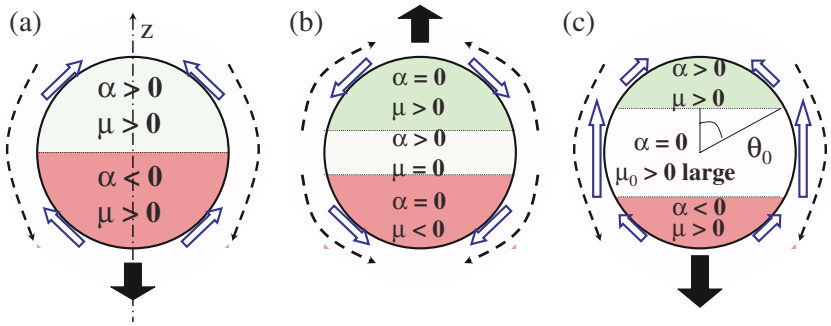

Figure 1. Three spherical swimmers described in the text. The flux of c (opposite to the gradient) is depicted with the dashed arrows, while the resulting slip velocity of the liquid along the sphere is described by open arrows. The net swimming direction is given by the thick dark arrow. (a) A Janus swimmer, with a homogeneous μ and a broken top-down symmetry in α: one hemisphere produces c while the other consumes it. (b) A Saturn swimmer with an equatorial belt producing c, and a broken symmetry in the phoretic mobility between the two hemispheres (here even opposite signs), which induce swimming in the same direction from the (opposite) equator to poles gradients. (c) A three-slice design in with polar slices efficient in producing and consuming c, while the equatorial slice is chosen for its large mobility. Properly choosing θ_0 permits maximization of the swimming velocity (figure 2).

and find

$$\mathbf{V} = \frac{4}{45}\frac{\mu_0\alpha_0}{D}\hat{\mathbf{e}}_z. \tag{11}$$

So symmetry breaking in mobility alone also leads to swimming: the activity at the equator generates gradients of c towards the poles that generate slip velocities in the same direction along z as the sign of μ is opposite on the two hemispheres (figure 1(b)).

The third design is that of a three-slice sphere, that illustrates typical considerations that arise when trying to increase by design the swimming velocity. From the scaling analysis above one should obviously aim for surfaces with both large values of α and μ. However, in many cases these goals will not be met by a single surface, so one may instead look for ways to combine in an efficient design surfaces with large α and surfaces with large μ. As an example, let us try to upgrade the Janus design of figure 1(a) by adding a passive belt of large phoretic mobility μ_0, which leads to the swimmer of figure 1(c):

$$(\alpha(\theta), \mu(\theta)) = \begin{cases} (\alpha_+, \mu_+), & 0 < \theta < \theta_+, \\ (0, \mu_0), & \theta_+ < \theta < \pi - \theta_-, \\ (\alpha_-, \mu_-), & \pi - \theta_- < \theta < \pi\,. \end{cases} \tag{12}$$

To reach the largest swimming velocity for given surface properties, one can adjust the values of θ_+ and θ_- in a compromise between increasing the mobility by enlarging the belt without shrinking too much the poles that generate the gradient. Figure 2 shows results for the model case $\alpha_+ = -\alpha_- = \alpha$, $\mu_+ = \mu_- = \mu$ of same sign than μ_0, $\theta_+ = \theta_- = \theta_0$: for $\mu_0 > \mu$ there is a

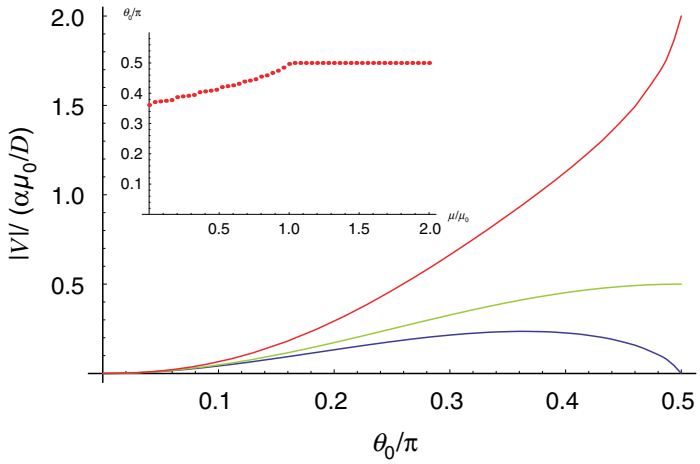

Figure 2. Reduced swimming velocity $V/(\alpha\mu_0/D)$ of the three-slice swimmer of figure 1(c), as a function of 'polar' angle θ_0 for various values of μ/μ_0: 0, 1, 4 (from bottom to top). The optimal value at low μ/μ_0 reflects the compromise between large poles to have strong chemical gradients, and a large equatorial belt for these gradients to translate into large flow motion. Inset: optimal angle θ_0 against μ/μ_0.

value of θ_0 that maximizes the speed, which is always larger than $\pi/3$, i.e. no matter how large μ_0, the 'optimal' belt should not be made larger than a fixed value. The relative flatness of the bottom curve in figure 2 shows a moderate dependence on θ_0 around this value, so that the swimming velocity should be rather robust to small imprecisions in the fabrication.

4. Thin rods

Because of the many experimental realizations of such systems [6, 7] we discuss the case of long cylindrical rods (length $2L$ and radius $b \ll L$) with surface properties varying only along their axis $-L \leqslant z \leqslant L$, i.e. $\mu = \mu(z)$, $\alpha = \alpha(z)$. In the limit $L \gg b$ slender body theory can be used, and remarkably equation (2) yields a simple form for the swimming velocity along z:

$$V \simeq -\frac{1}{2L}\int_{-L}^{L} \mathrm{d}z\ \mu(z)\partial_z c_\mathrm{s}. \tag{13}$$

In the same limit, the surface concentration c_s is related to the surface activity $\alpha(z)$ by [6]

$$c_\mathrm{s}(z) \simeq \frac{b}{2D}\int_{-L}^{L} \mathrm{d}z'\ \frac{\alpha(z')}{|z-z'|}. \tag{14}$$

These two equations give the velocity of a rod for any 'bar-coded' surface properties α and μ. For a Janus rod

$$(\alpha(z), \mu(z)) = \begin{cases} (\alpha_-, \mu_-), & -L < z < 0, \\ (\alpha_+, \mu_+), & 0 < z < L, \end{cases} \tag{15}$$

we find

$$V = \frac{1}{4D}\left(\frac{b}{L}\right)\ln\left(\frac{L}{4b}\right)(\mu_+\alpha_- - \mu_-\alpha_+)\,, \tag{16}$$

which illustrates a few important points: (i) again swimming is obtained by symmetry breaking in the chemical activity or/and in the phoretic mobility, (ii) swimming with uniform activity ($\alpha =$ constant) is possible, in contrast to the special case of spheres for which this leads to no tangential gradients of c, (iii) the velocity scale is decreased by a factor of $\sim b/L$ when compared to a sphere of radius $\sim L$, because the surface generated flux of c is reduced by a similar factor, and (iv) V is up to logarithms proportional to $1/L$ at fixed rod diameter, but scale independent if length and diameter are varied in the same proportion.

5. Discussion

The swimming velocity V of a phoretic swimmer, is independent of its size and scales as $V \sim \alpha\mu/D$, where α and μ are averages quantifying the surface activity generating the gradient and the surface phoretic mobility. The exact value of V depends on the shape and surface pattern in a computable way. For example, spheres swim faster than rods of same longest dimension, and improvement can be obtained by properly combining various types of surfaces.

1. This type of formalism holds for self-diffusiophoresis (with α the surface reaction density, μ the diffusiophoretic mobility, and D the solute diffusion coefficient), for self-electrophoresis (with α the electrical current density injected in the solution, μ the electrophoretic mobility, and D the solution electrical conductivity), and for self-thermophoresis (with α the surface heat flux injected in the solution, μ the thermophoretic mobility, and D the solution thermal conductivity). As for motion driven by external gradients, the largest velocities are expected for highly charged surfaces at low ionic strengths, which yield large mobilities μ because of the thick interfacial electrical double-layer.
2. The present line of reasoning can be adapted to more accurate descriptions of surface chemistry for specific experimental conditions. What is required in a given situation is an appropriate scheme for computing $\alpha(\mathbf{r}_s)$. For example if c is produced at the surface from some chemical at concentration $c^\infty_{\rm fuel}$ far away from the object, various regimes show up. We have focused on kinetics limited by the number of catalytic sites on the surface, but for low values of $c^\infty_{\rm fuel}$ the reaction becomes diffusion limited so that α depends on the global geometry.
3. Due to thermal rotational diffusion, if no external field orients the objects, the direction of motion persists only for a time $\tau \simeq 1/D_{\rm rot}$, where $D_{\rm rot} \simeq k_{\rm B}T/\eta R^3$ and R is the largest dimension of the object. Note however that the field c typically adjusts much faster to a change of orientation ($R^2/D \ll 1/D_{\rm rot}$), so our steady-state estimates still hold for the instantaneous velocity. A simple Langevin dynamics with a diffusion coefficient $D_{\rm trans} \sim k_{\rm B}T/\eta R$ and drift at V along a stochastically changing direction ($D_{\rm rot} = 1/\tau$) leads to diffusive behaviour at long times ($t \gg \tau$) with an activity-enhanced diffusion coefficient $D_{\rm eff} = D_{\rm trans} + \frac{1}{6}V^2\tau$. This enhancement may be significant and measurable for not too small swimmers, i.e. $R > (k_{\rm B}T/\eta V)^{1/2}$, of order $\sim$ a few 100 nm for $V \sim 10\,\mu$m s^{-1} in water.

   For nano-rods of radius b fixed due to fabrication constraints [6], the scaling of the previous quantities become (using the shorthand $V_0 = \alpha/\mu D$ and forgetting

logarithms) $V \simeq V_0(b/L)$, $\tau \sim \eta L^3/k_B T$, and an activity-induced enhancement of the bare translational coefficient $D_{trans} \sim k_B T/\eta L$ by a quantity $\sim (\eta V_0^2/k_B T)b^2 L$, significant if $L/b > (k_B T/\eta V_0 b^2)$.

4. Beyond the 'linear' swimmers described here, our approach can also describe active 'spinners,' which rotate using the same mechanisms [6, 7]. Their angular velocity can be computed by replacing (4) by the formula for angular swimming speed given in [12], and scales as $\Omega \sim \alpha\mu/DR$, decreasing with object size for a given shape and geometrical surface pattern.
5. There is a growing interest in the collective behaviour of swimming organisms (see e.g. [17] and references therein). Phoretic swimmers are special with regards to these questions as they interact through both their hydrodynamic fields (decaying as the inverse of the cube of their relative distance r^{-3}) [2] and the c-field gradients they generate (which decay as r^{-2} for a net production/absorption of c per object, and as r^{-3} otherwise).

In conclusion, we have provided generic considerations for the design of small phoretic swimmers (size (in)dependence of the swimming velocity, necessary symmetry breaking in the surface pattern), as well as quantitative procedures to estimate the influence of their velocity. Beyond these considerations, fast motion of course relies on clever surface engineering to obtain large surface 'activity' and 'phoretic mobility.' We hope that our calculations will stimulate experimental studies of swimmers with given surface chemistries but various surface patterns, e.g. nanorods [6, 7] and spheres [11, 18] keeping in mind that other effects (e.g. bubble generation [7]) may compete with the ones described here.

References

[1] Dreyfus R, Baudry J, Roper M L, Fermigier M, Stone H A and Bibette J 2005 *Nature* **437** 862
[2] Anderson J L 1989 *Ann. Rev. Fluid Mech.* **21** 61
[3] Mitchell P 1972 *FEBS Lett.* **28** 1
[4] Lammert P, Prost J and Bruinsma R 1996 *J. Theor. Biol.* **178** 387
[5] Golestanian R, Liverpool T B and Ajdari A 2005 *Phys. Rev. Lett.* **94** 220801
[6] Paxton W F, Sen A and Mallouk T E 2005 *Chem.—Eur. J.* **11** 6462
Paxton W F *et al* 2004 *J. Am. Chem. Soc.* **126** 13424
[7] Ozin G A, Manners I, Fournier-Bidoz S and Arsenault A 2005 *Adv. Mater.* **17** 3011
Fournier-Bidoz S, Arsenault A, Manners I and Ozin G A 2005 *Chem. Commun.* **4** 441
[8] Vicario J, Eelkema R, Browne W R, Meetsma A, La Crois R M and Feringa B L 2005 *Chem. Commun.* **4** 3936
[9] Mano N and Heller A 2005 *J. Am. Chem. Soc.* **127** 11575
[10] Wang Y, Hernandez R M, Bartlett D J Jr, Bingham J M, Kline T R, Sen A and Mallouk T E 2006 *Langmuir* **22** 10451
[11] Perro A, Reclusa S, Ravaine S, Bourgeat-Lami E and Duguet E 2005 *J. Mater. Chem.* **15** 3745
[12] Stone H A and Samuel A 1996 *Phys. Rev. Lett.* **77** 4102
[13] Happel J and Brenner H 1965 *Low Reynolds Number Hydrodynamics* (Englewood Cliffs, NJ: Prentice-Hall)
[14] Kim Y W and Netz R R 2005 *Europhys. Lett.* **72** 837
[15] Ajdari A and Bocquet L 2006 *Phys. Rev. Lett.* **96** 186102
[16] Anderson J L 1985 *J. Colloid Interface Sci.* **105** 45
[17] Hernandez-Ortiz J, Stoltz C G and Graham M D 2005 *Phys. Rev. Lett.* **95** 204501
[18] Howse J R, Jones R A L, Ryan A J, Gough T, Vafabakhsh R and Golestanian R 2006 *Preprint*